

# A Younger Age for the Universe

Charles H. Lineweaver

School of Physics, University of New South Wales, Sydney NSW 2052, Australia  
charley@bat.phys.unsw.edu.au

## ABSTRACT

The age of the universe in the Big Bang model can be calculated from three parameters: Hubble's constant,  $h$ ; the mass density of the universe,  $\Omega_m$ ; and the cosmological constant,  $\Omega_\Lambda$ . Recent observations of the cosmic microwave background and six other cosmological measurements reduce the uncertainty in these three parameters, yielding an age for the universe of  $13.4 \pm 1.6$  billion years, which is a billion years younger than other recent age estimates. A different standard Big Bang model, which includes cold dark matter with a cosmological constant, provides a consistent and absolutely time-calibrated evolutionary sequence for the universe.

In the Big Bang model, the age of the universe,  $t_o$ , is a function of three parameters:  $h$ ,  $\Omega_m$  and  $\Omega_\Lambda$  (1). The dimensionless Hubble constant,  $h$ , tells us how fast the universe is expanding. The density of matter in the universe,  $\Omega_m$ , slows the expansion, and the cosmological constant,  $\Omega_\Lambda$ , speeds up the expansion (Fig. 1).

Until recently, large uncertainties in the measurements of  $h$ ,  $\Omega_m$  and  $\Omega_\Lambda$  made efforts to determine  $t_o(h, \Omega_m, \Omega_\Lambda)$  unreliable. Theoretical preferences were, and still are, often used to remedy these observational uncertainties. One assumed the standard model ( $\Omega_m = 1$ ,  $\Omega_\Lambda = 0$ ), dating the age of the universe to  $t_o = 6.52/h$  billion years old (Ga). However, for large or even moderate  $h$  estimates ( $\gtrsim 0.65$ ), these simplifying assumptions resulted in an age crisis in which the universe was younger than our Galaxy ( $t_o \approx 10 \text{ Ga} < t_{Gal} \approx 12 \text{ Ga}$ ). These assumptions also resulted in a baryon crisis in which estimates of the amount of normal (baryonic) matter in the universe were in conflict (2, 3).

Evidence in favor of  $\Omega_m < 1$  has become more compelling (4-8), but  $\Omega_\Lambda$  is still often assumed to be zero, not because it is measured to be so, but because models are simpler without it. Recent evidence from supernovae (SNe) (4, 5) indicates that  $\Omega_\Lambda > 0$ . These SNe data and other data exclude the standard Einstein-deSitter model ( $\Omega_m = 1$ ,  $\Omega_\Lambda = 0$ ). The cosmic microwave background (CMB), on the other hand, excludes models with low  $\Omega_m$  and  $\Omega_\Lambda = 0$  (3). With both high and low  $\Omega_m$  excluded,  $\Omega_\Lambda$  cannot be zero. Combining CMB measurements with SNe and other data, I (9) have reported  $\Omega_\Lambda = 0.62 \pm 0.16$ . [see (10-12) for similar results]. If  $\Omega_\Lambda \neq 0$ , then estimates of the age of the universe in Big Bang models must include  $\Omega_\Lambda$ . Thus one must use the most general form:  $t_o = f(\Omega_m, \Omega_\Lambda)/h$  (13).

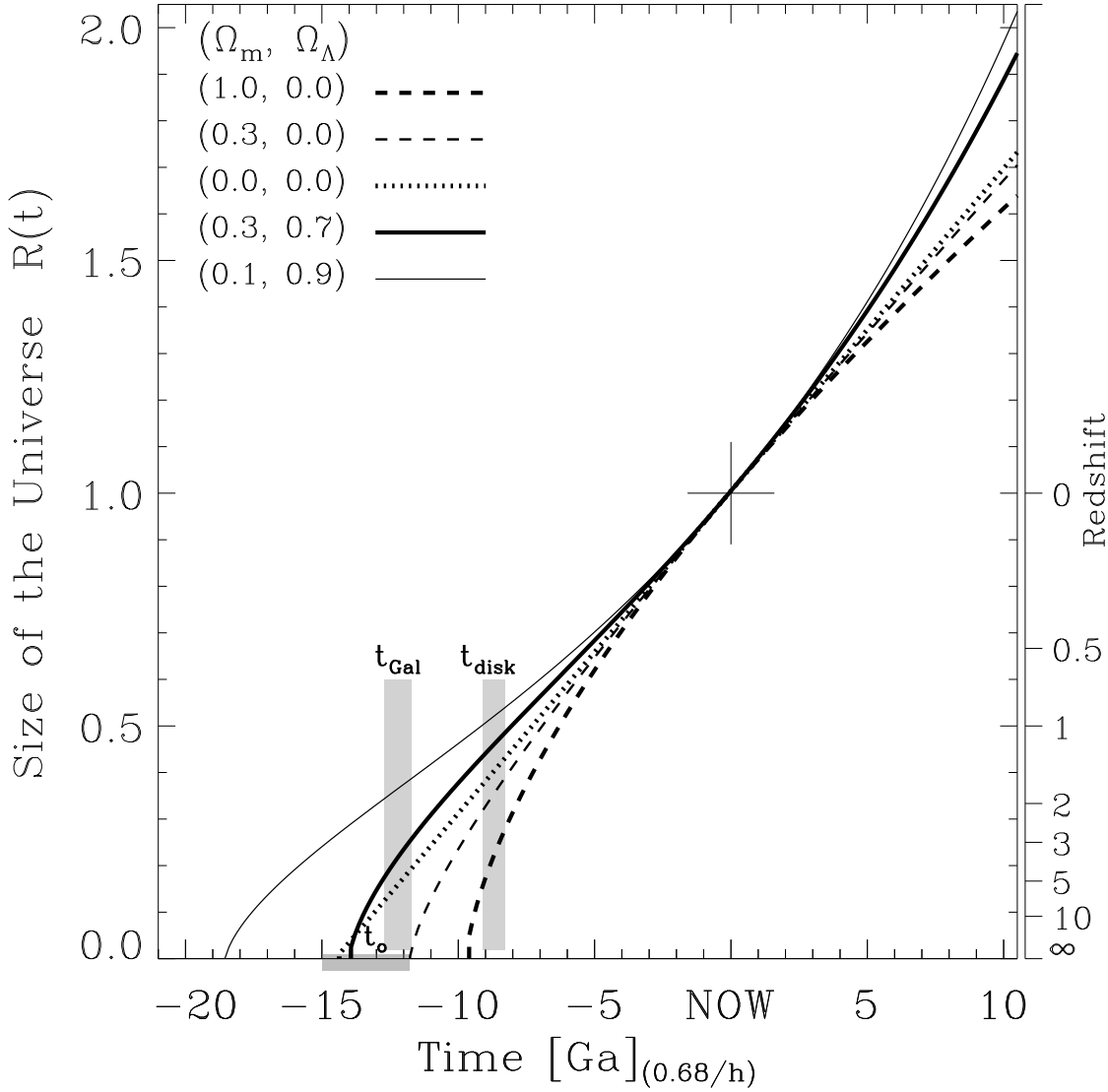


Fig. 1.— The size of the universe, in units of its current size, as a function of time. The age of the five models can be read from the x axis as the time between NOW and the intersection of the model with the x axis. The main result of this paper,  $t_o = 13.4 \pm 1.6$  Ga, is labeled “ $t_o$ ” and is shaded gray on the x axis. Measurements of the age of the halo of our Galaxy yield  $t_{\text{Gal}} = 12.2 \pm 0.5$  Ga, whereas measurements of the age of the disk of our Galaxy yield  $t_{\text{disk}} = 8.7 \pm 0.4$  Ga (Table 2). These age ranges are also labeled and shaded gray. The  $(\Omega_m, \Omega_\Lambda) = (0.3, 0.7)$  model fits the constraints of Table 1 better than the other models shown. Over the past few billion years and on into the future, the rate of expansion of this model increases ( $\ddot{R} > 0$ ). This acceleration means we are in a period of slow inflation. Other consequences of a  $\Omega_\Lambda$ -dominated universe are discussed in (50). On the x axis  $h = 0.68$  has been assumed. For other values of  $h$ , multiply the x axis ages by  $0.68/h$ . Redshifts are indicated on the right.

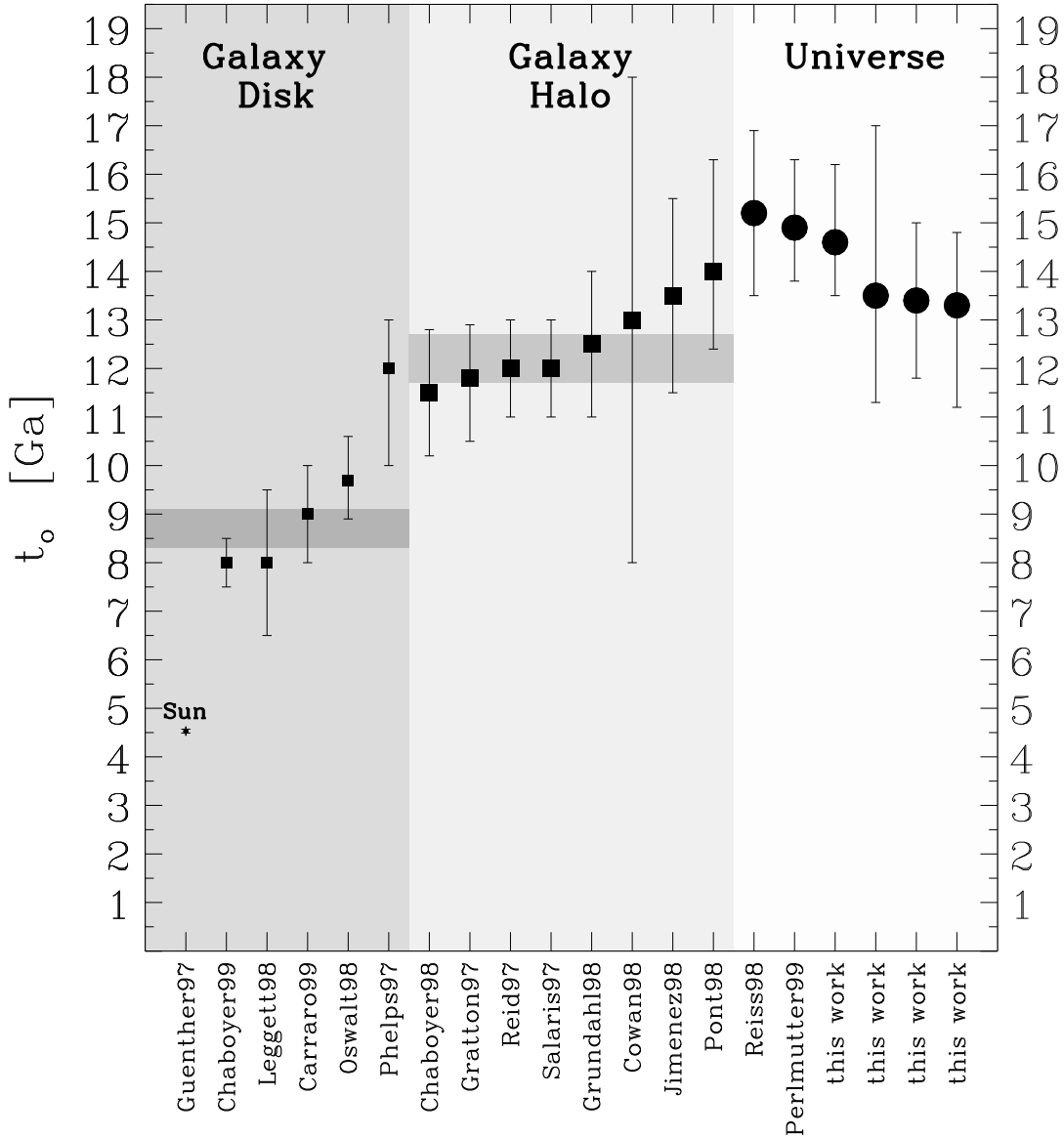


Fig. 2.— Age estimates of the universe and of the oldest objects in our Galaxy. The four estimates of the age of the universe from this work are indicated in Table 2. The three similar points near 13.4 Ga, result from  $h = 0.64, 0.68, 0.72$  and indicate that the result is not strongly dependent on  $h$  when a reasonable  $h$  uncertainty of  $\pm 0.10$  is used. Among the four, the highest value at 14.6 Ga comes from assuming  $h = 0.64 \pm 0.02$ . All the estimates in the top section of Table 2 are plotted here. As in Fig. 1, averages of the ages of the Galactic halo and Galactic disk are shaded gray. The absence of any single age estimate more than  $\sim 2\sigma$  from the average adds plausibility to the possibly overdemocratic procedure of computing the variance-weighted averages. The result that  $t_o > t_{\text{Gal}}$  is logically inevitable, but the standard Einstein-deSitter model does not satisfy this requirement unless  $h < 0.55$ . The reference for each measurement is given under the x axis. The age of the sun is accurately known and is included for reference. Error bars indicate the reported  $1\sigma$  limits.

Table 1: Parameter estimates from non-CMB measurements. I refer to these as constraints. I use the error bars cited here as  $1\sigma$  errors in the likelihood analysis. The first four constraints are plotted in Fig. 3 B through E.

Method	Reference	Estimate	
SNe	(35)	$\Omega_m^{\Lambda=0} = -0.28 \pm 0.16$	$\Omega_m^{\text{flat}} = 0.27 \pm 0.14$
Cluster mass-to-light	(6)	$\Omega_m^{\Lambda=0} = 0.19 \pm 0.14$	
Cluster abundance evolution	(7)	$\Omega_m^{\Lambda=0} = 0.17^{+0.28}_{-0.10}$	$\Omega_m^{\text{flat}} = 0.22^{+0.25}_{-0.10}$
Double radio sources	(8)	$\Omega_m^{\Lambda=0} = -0.25^{+0.70}_{-0.50}$	$\Omega_m^{\text{flat}} = 0.1^{+0.50}_{-0.20}$
Baryons	(19)	$\Omega_m h^{2/3} = 0.19 \pm 0.12$	
Hubble	(16)	$h = 0.68 \pm 0.10$	

Here I have combined recent independent measurements of CMB anisotropies (9), type Ia SNe (4, 5), cluster mass-to-light ratios (6), cluster abundance evolution (7), cluster baryonic fractions (14), deuterium-to-hydrogen ratios in quasar spectra (15), double-lobed radio sources (8), and the Hubble constant (16) to determine the age of the universe. The big picture from the analysis done here is as follows (Figs. 1 and 2): The Big Bang occurred at  $\sim 13.4$  Ga. About 1.2 billion years (Gy) later, the halo of our Galaxy (and presumably the halo of other galaxies) formed. About 3.5 Gy later, the disk of our Galaxy (and presumably the disks of other spiral galaxies) formed. This picture agrees with what we know about galaxy formation. Even the recent indications of the existence of old galaxies at high redshift (17) fit into the time framework determined here. In this sense, the result is not surprising. What is new is the support given to such a young age by such a wide array of recent independent measurements.

### Method

Any measurement of a function of  $h, \Omega_m$ , and  $\Omega_\Lambda$  can be included in a joint likelihood

$$\mathcal{L}(h, \Omega_m, \Omega_\Lambda) = \prod_{i=1}^N \mathcal{L}_i \quad (1)$$

which I take as the product of seven of the most recent independent cosmological constraints (Table 1 and Fig. 3). For example, one of the  $\mathcal{L}_i$  in Eq. 1 represents the constraints on  $h$ . Recent measurements can be summarized as  $\bar{h} = 0.68 \pm 0.10$  (16). I represent these measurements in Eq. 1 by the likelihood,

$$\mathcal{L}_{\text{Hubble}}(h) = \exp \left[ -0.5 \left( \frac{h - \bar{h}}{0.10} \right)^2 \right] \quad (2)$$

Another  $\mathcal{L}_i$  in Eq. 1 comes from measurements of the fraction of normal baryonic matter in clusters of galaxies (14) and estimates of the density of normal baryonic matter in the

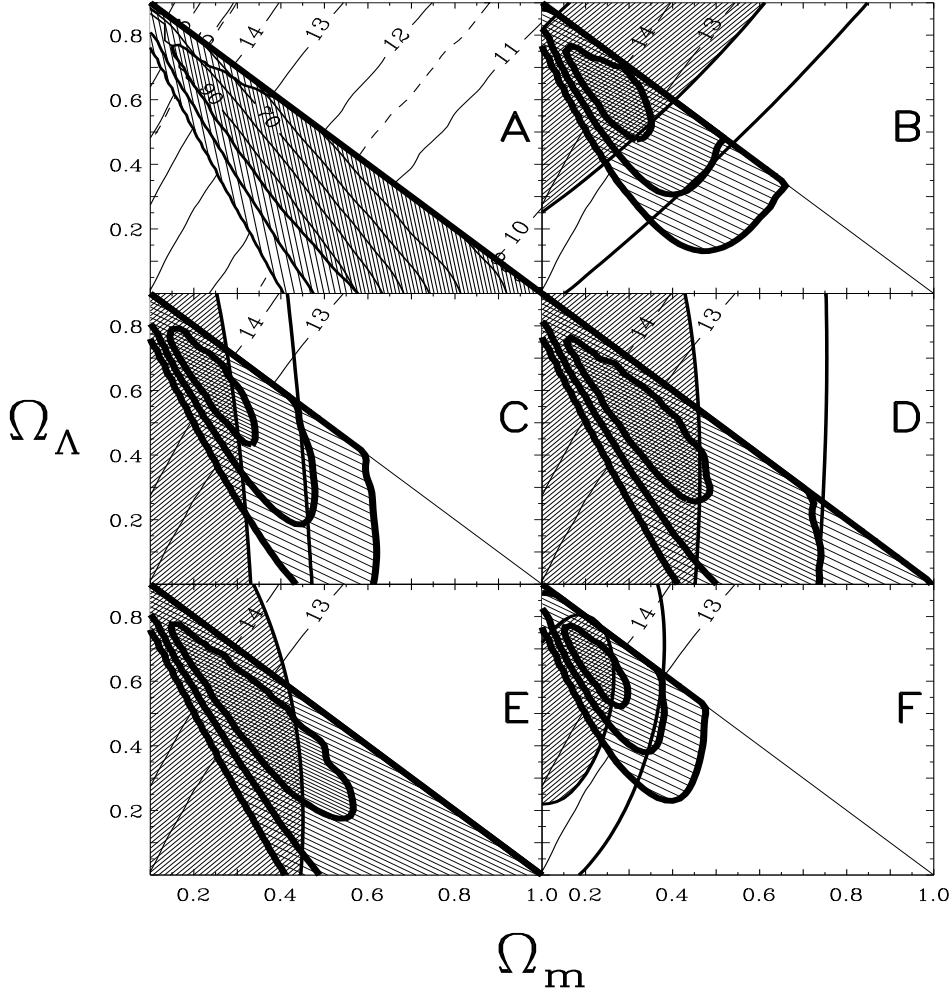


Fig. 3.— The regions of the  $(\Omega_m, \Omega_\Lambda)$  plane preferred by various constraints. (A) Cosmic microwave background, (B) SNe, (C) cluster mass-to-light ratios, (D) cluster abundance evolution, (E) double radio lobes, and (F) all combined. The power of combining CMB constraints with each of the other constraints (Table 1) is also shown. The elongated triangles (from upper left to lower right) in (A) are the approximate  $1\sigma$ ,  $2\sigma$  and  $3\sigma$  confidence levels of the likelihood from CMB data,  $\mathcal{L}_{\text{CMB}}$  (9). (A) also shows the important  $h$  dependence of  $\mathcal{L}_{\text{CMB}}$ . The contours within the dark shaded region are of  $h$  values that maximize  $\mathcal{L}_{\text{CMB}}$  for a given  $(\Omega_m, \Omega_\Lambda)$  pair ( $h = 0.70, 0.90$  contours are labeled). This correlation between preferred  $h$  and preferred  $(\Omega_m, \Omega_\Lambda)$  helps  $\mathcal{L}_{\text{CMB}}(h, \Omega_m, \Omega_\Lambda)$  constrain  $t_o$ . In (B) through (E), thin contours enclose the  $1\sigma$  (shaded) and  $2\sigma$  confidence regions from separate constraints, and thick contours indicate the  $1\sigma$ ,  $2\sigma$  and  $3\sigma$  regions of the combination of  $\mathcal{L}_{\text{CMB}}$  with these same constraints. (F) shows the region preferred by the combination of the separate constraints shown in (B) through (E) (thin contours) as well as the combination of (A) through (E) (thick contours). The best fit values are  $\Omega_\Lambda = 0.65 \pm 0.13$  and  $\Omega_m = 0.23 \pm 0.08$ . In (A), the thin iso- $t_o$  contours (labeled “10” through “14”) indicate the age in Ga when  $h = 0.68$  is assumed. For reference, the 13- and 14-Ga contours are in all the panels. To give an idea of the sensitivity of the  $h$  dependence of these contours, the two additional dashed contours in (A) show the 13-Ga contours for  $h = 0.58$  and  $h = 0.78$  (the  $1\sigma$  limits of the principle  $h$  estimate used in this paper). In (F), it appears that the best fit has  $t_o \approx 14.5$  Ga, but all constraints shown here are independent of information about  $h$ ; they do not include the  $h$  dependence of  $\mathcal{L}_{\text{CMB}}$ ,  $\mathcal{L}_{\text{baryons}}$  or  $\mathcal{L}_{\text{Hubble}}$  (Table 1).

universe [ $\Omega_b h^2 = 0.015 \pm 0.005$  (15, 18)]. When combined, these measurements yield  $\overline{\Omega_m h^{2/3}} = 0.19 \pm 0.12$  (19), which contributes to the likelihood through

$$\mathcal{L}_{baryons}(h, \Omega_m) = \exp \left[ -0.5 \left( \frac{\Omega_m h^{2/3} - \overline{\Omega_m h^{2/3}}}{0.12} \right)^2 \right] \quad (3)$$

The  $(\Omega_m, \Omega_\Lambda)$ -dependencies of the remaining five constraints are plotted in Fig. 3 (20). The 68% confidence level regions derived from CMB and SNe (Fig. 3, A and B) are nearly orthogonal, and the region of overlap is relatively small. Similar complementarity exists between the CMB and the other data sets (Figs. 3, C through E). The combination of them all (Fig. 3F) yields  $\Omega_\Lambda = 0.65 \pm 0.13$  and  $\Omega_m = 0.23 \pm 0.08$  (21).

This complementarity is even more important (but more difficult to visualize) in three-dimensional parameter space:  $(h, \Omega_m, \Omega_\Lambda)$ . Although the CMB alone cannot tightly constrain any of these parameters, it does have a strong preference in the three-dimensional space  $(h, \Omega_m, \Omega_\Lambda)$ . In Eq. 1, I used  $\mathcal{L}_{CMB}(h, \Omega_m, \Omega_\Lambda)$ , which is a generalization of  $\mathcal{L}_{CMB}(\Omega_m, \Omega_\Lambda)$  (Fig. 3A )(22). To convert the three-dimensional likelihood  $\mathcal{L}(h, \Omega_m, \Omega_\Lambda)$  of Eq. 1 into an estimate of the age of the universe and into a more easily visualized two-dimensional likelihood,  $\mathcal{L}(h, t_o)$ , I computed the dynamic age corresponding to each point in the three-dimensional space  $(h, \Omega_m, \Omega_\Lambda)$ . For a given  $h$  and  $t_o$ , I then set  $\mathcal{L}(h, t_o)$  equal to the maximum value of  $\mathcal{L}(h, \Omega_m, \Omega_\Lambda)$

$$\mathcal{L}(h, t_o) = \max \left[ \mathcal{L}(h, \Omega_m, \Omega_\Lambda) |_{t(h, \Omega_m, \Omega_\Lambda) \approx t_o} \right] \quad (4)$$

This has the advantage of explicitly displaying the  $h$  dependence of the  $t_o$  result. The joint likelihood  $\mathcal{L}(h, t_o)$  of Eq. 4 yields an age for the universe:  $t_o = 13.4 \pm 1.6$  Ga (Fig. 4). This result is a billion years younger than other recent age estimates.

What one uses for  $\mathcal{L}_{Hubble}(h)$  in Eq. 1 is particularly important because, in general, we expect the higher  $h$  values to yield younger ages. Table 2 contains results from a variety of  $h$  estimates, assuming various central values and various uncertainties around these values. The main result  $t_o = 13.4 \pm 1.6$  Ga has used  $h = 0.68 \pm 0.10$  but does not depend strongly on the central value assumed for Hubble's constant (as long as this central value is in the most accepted range,  $0.64 \leq h \leq 0.72$ ) or on the uncertainty of  $h$  (unless this uncertainty is taken to be very small). Assuming an uncertainty of 0.10, age estimates from using  $h = 0.64, 0.68$  and  $0.72$  are 13.5, 13.4 and 13.3 Ga, respectively (Fig. 2). Using a larger uncertainty of 0.15 with the same  $h$  values does not substantially change the results, which are 13.4, 13.3, 13.2 Ga, respectively. For both groups, the age difference is only 0.2 Gy. If  $t_o \propto 1/h$  were adhered to, this age difference would be 1.6 Gy. Outside the most accepted range the  $h$  dependence becomes stronger and approaches  $t_o \propto 1/h$  (23).

To show how each constraint contributes to the result, I convolved each constraint separately with Eq. 2 (Fig. 5). The result does not depend strongly on any one of the constraints (see "all - x" results in Table 2). For example, the age, independent of the SNe

data, is  $t_o(all - SNe) = 13.3_{-1.8}^{+1.7}$  Ga, which differs negligibly from the main result. The age, independent of the SNe and CMB data, is  $t_o(all - CMB - SNe) = 12.6_{-2.0}^{+3.4}$  Ga, which is somewhat lower than the main result but within the error bars.

### The Oldest Objects in Our Galaxy

The universe cannot be younger than the oldest objects in it. Thus, estimates of the age of the oldest objects in our Galaxy are lower limits to the age of the universe (Table 2 and Fig. 2). A standard but simplified scenario for the origin of our Galaxy has a halo of globular clusters forming first, followed by the formation of the Galactic disk. The most recent measurements of the age of the oldest objects in the Galactic disk give  $t_{disk} = 8.7 \pm 0.4$  Ga (Table 2). The most recent measurements of the age of the oldest objects in the halo of our Galaxy give  $t_{Gal} = 12.2 \pm 0.5$  Ga (Table 2). The individual measurements are in good agreement with these averages. There are no large outliers. In contrast to the  $t_o(h, \Omega_m, \Omega_\Lambda)$  estimates obtained above, all of these age estimates are direct in the sense that they have no dependence on a Big Bang model.

How old was the universe when our Galaxy formed? If we write this as  $t_{Gal} + \Delta t = t_o$ , then what is the amount of time ( $\Delta t$ ) between the formation of our Galaxy and the formation of the universe? If we had an estimate of  $\Delta t$ , then we would have an independent estimate of  $t_o$  to compare to  $t_o = 13.4 \pm 1.6$  Ga, obtained above. However, we have very poor constraints on  $\Delta t$ . The simple but plausible estimate  $\Delta t \approx 1$  Gy is often invoked, but estimates range from  $\sim 0.1$  to  $\sim 5$  Gy, and may be even larger (24, 25). This uncertainty in  $\Delta t$  undermines the ability of estimates of the age of the oldest objects in our Galaxy to tell us the age of the universe. Without  $\Delta t$ , we cannot infer  $t_o$  from  $t_{Gal}$ . The best estimate of  $\Delta t$  may come from the difference between the age reported here and the estimate of the age of our Galaxy (Table 2). Thus  $\Delta t = t_o - t_{Gal} = 13.4 - 12.2 = 1.2 \pm 1.8$  Gy.

The age measurements in Table 2 also indicate that there is a 3.5-Gy period between halo and disk formation ( $t_{Gal} - t_{disk}$ ). If our Milky Way is typical, then this may be true of other spiral galaxies. With the best fit values obtained here for the three parameters,  $(h, \Omega_m, \Omega_\Lambda) = (0.72 \pm 0.09, 0.23 \pm 0.08, 0.65 \pm 0.13)$ , the ages  $t_{disk}$  and  $t_{Gal}$  can be converted into the redshifts at which the disk and halo formed:  $z_{disk} = 1.3_{-0.5}^{+1.5}$  and  $z_{Gal} = 6.0_{-4.3}^{+\infty}$ . Thus, a diskless epoch should be centered at a redshift between  $z_{disk}$  and  $z_{Gal}$  ( $1.3 \lesssim z_{diskless} \lesssim 6.0$ ). We would expect fewer disks in the halolike progenitors of spiral galaxies in this redshift range. Studies of galaxy types in the Hubble Deep Field indicate that this may be the case (26).

The requirement that the universe be older than our Galaxy,  $t_o > t_{Gal}$ , is a consistency test of the Big Bang model. The best fit model obtained here passes this test. There is no age crisis. This is true even if the high values of  $h$  ( $\sim 0.80$ ) are correct. Only at  $h \approx 0.85$  is  $t_o \approx t_{Gal}$ . This consistency provides further support for the Big Bang model, which the standard model ( $\Omega_m = 1, \Omega_\Lambda = 0$ ) is unable to match unless  $h < 0.55$ .

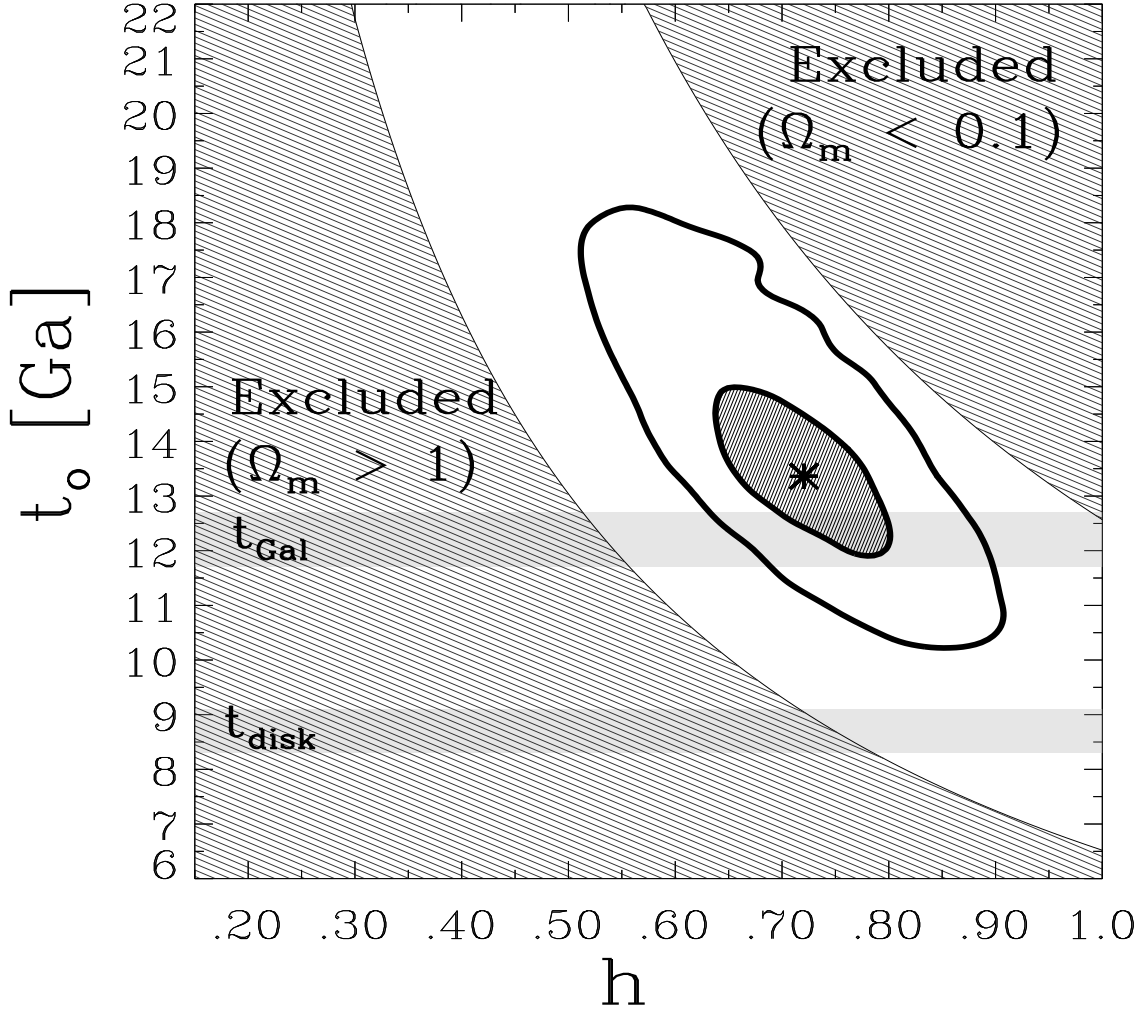


Fig. 4.— This plot shows the region of the  $h - t_0$  plane preferred by the combination of all seven constraints. The result,  $t_0 = 13.4 \pm 1.6$  Ga, is the main result of this paper. The thick contours around the best fit (indicated by a star) are at likelihood levels defined by  $\mathcal{L}/\mathcal{L}_{\text{max}} = 0.607$ , and 0.135, which approximate 68% and 95% confidence levels, respectively. These contours can be projected onto the  $t_0$  axis to yield the age result. This age result is robust to variations in the Hubble constraint as indicated in Table 2. The areas marked “Excluded” (here and in Fig. 5) result from the range of parameters considered:  $0.1 \leq \Omega_m \leq 1.0$ ,  $0 \leq \Omega_\Lambda \leq 0.9$  with  $\Omega_m + \Omega_\Lambda \leq 1$ . Thus, the upper (high  $t_0$ ) boundary is defined by  $(\Omega_m, \Omega_\Lambda) = (0.1, 0.9)$ , and the lower boundary is the standard Einstein-deSitter model defined by  $(\Omega_m, \Omega_\Lambda) = (1, 0)$ . Both of these boundary models are plotted in Fig. 1. The estimates from Table 2 of the age of our Galactic halo ( $t_{\text{Gal}}$ ) and the age of the Milky Way ( $t_{\text{disk}}$ ) are shaded grey. The universe is about 1 billion years older than our Galactic halo. The combined constraints also yield a best fit value of the Hubble constant which can be read off of the x axis ( $h = 0.73 \pm 0.09$ , a slightly higher and tighter estimate than the input  $h = 0.68 \pm 0.10$ ).



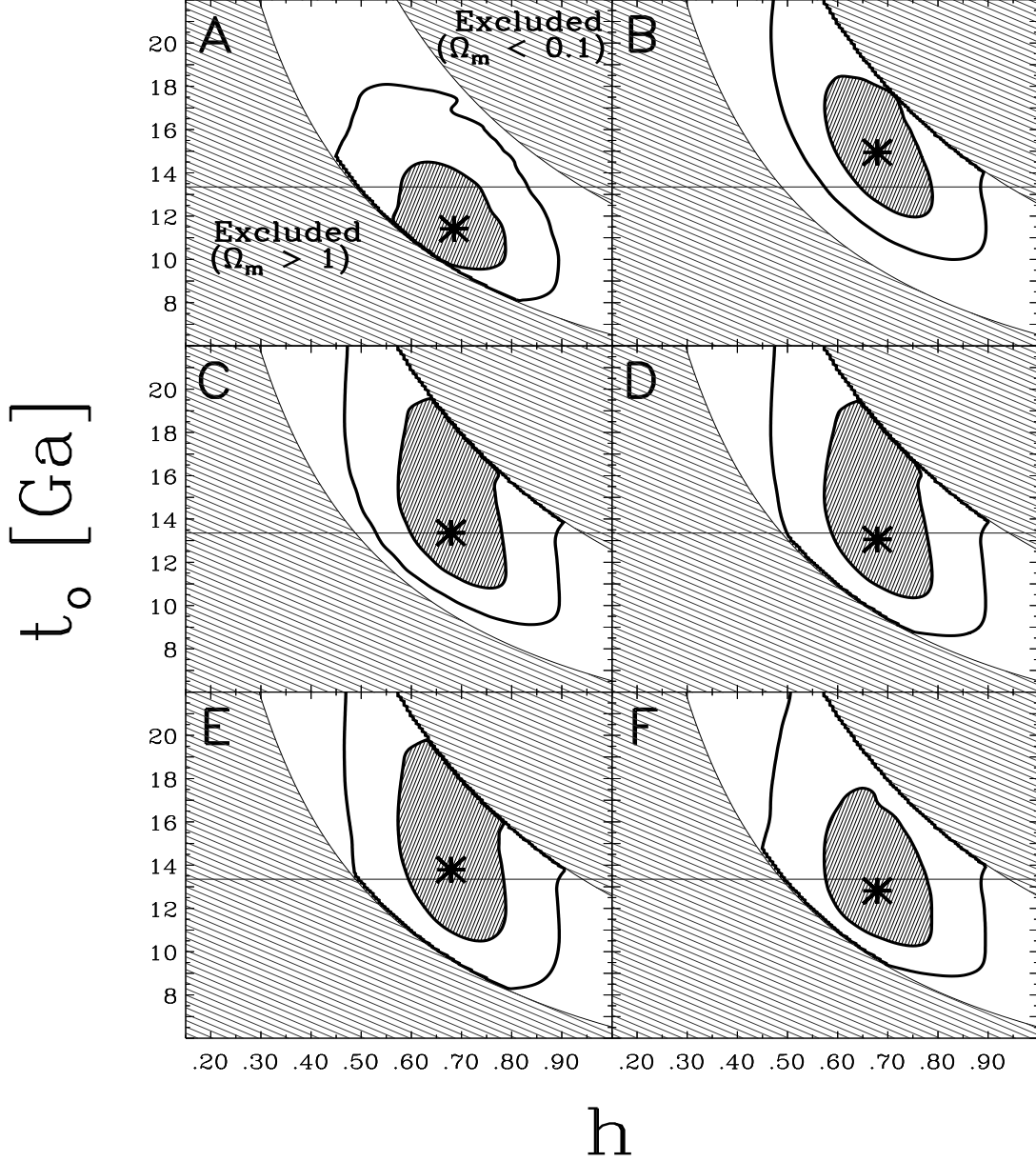


Fig. 5.— The purpose of this figure is to show how Fig. 4 is built up from the seven independent constraints used in the analysis. All six panels are analogous to Fig. 4 but contain only the Hubble constraint [ $h = 0.68 \pm 0.10$ , (Eq. 2)] convolved with a single constraint: (A) cosmic microwave background, (B) SNe, (C) cluster mass-to-light ratios, (D) cluster abundance evolution, (E) double radio lobes, and (F) baryons (Table 1). The relative position of the best fit (indicated by a star) and the 13.4-Ga line indicates how each constraint contributes to the result.

### Comparison with Previous Work

The goal of this paper is to determine the absolute age of the universe  $t_o(h, \Omega_m, \Omega_\Lambda)$ . Knowledge of  $h$  alone cannot be used to determine  $t_o$  with much accuracy. For example, the estimate  $h = 0.68 \pm 0.10$  corresponds to  $8 < t_o < 22$  Ga (Fig. 4). Similarly, knowledge of  $(\Omega_m, \Omega_\Lambda)$  yields  $H_o t_o(\Omega_m, \Omega_\Lambda)$  not  $t_o$  ( $H_o$  is the usual Hubble constant). When one inserts a preferred value of  $h$  into a  $H_o t_o$  result, one is not taking into consideration the correlations between preferred  $h$  values and preferred  $(\Omega_m, \Omega_\Lambda)$  values that are inherent, for example, in  $\mathcal{L}_{CMB}(h, \Omega_m, \Omega_\Lambda)$  and  $\mathcal{L}_{baryons}(h, \Omega_m)$ . The preferred values of  $h$  in these likelihoods depend on  $\Omega_m$  and  $\Omega_\Lambda$ . Perlmutter *et al.*(4) used SNe measurements to constrain  $(\Omega_m, \Omega_\Lambda)$  and obtained values for  $H_o t_o$ . To obtain  $t_o$ , they did the analysis with  $h$  set equal to the value preferred by their SNe data,  $h = 0.63$ . Their result is  $t_o = 14.5 \pm 1.0(0.63/h)$  Ga. When a flat universe is assumed, they obtain  $t_o^{flat} = 14.9_{-1.1}^{+1.4}(0.63/h)$  Ga. Riess *et al.*(5) found  $h = 0.65 \pm 0.02$  from their SNe data. Marginalizing over this Hubble value and over  $\Omega_\Lambda$  and  $\Omega_m$ , they report  $t_o = 14.2 \pm 1.7$  Ga. When a flat universe is assumed, their results yield  $t_o^{flat} = 15.2 \pm 1.7$  Ga. The Perlmutter *et al.*(4) and Riess (5) results are in good agreement. When I assume  $h = 0.64 \pm 0.02$ , I get  $t_o = 14.6_{-1.1}^{+1.6}$  Ga. This result is plotted in Fig. 2 to illustrate the important influence on the result of using a small  $h$  uncertainty. Efstathiou *et al.*(12), on the basis of a combination of CMB and Perlmutter *et al.*(4) SNe data, have estimated  $t_o = 14.6(h/0.65)^{-1}$  Ga. I used  $h = 0.65 \pm 0.0$  with this data combination to get  $t_o = 14.5_{-1.0}^{+1.2}$  Ga. However, when I used  $h = 0.65 \pm 0.10$ , the result is 0.7 Gy lower ( $t_o = 13.8_{-1.4}^{+3.2}$  Ga). To obtain the main result, I used uncertainties large enough to reflect our knowledge of  $h$  on the basis of many sources. The use of a larger  $h$  uncertainty contributes to the substantially younger ages found here (23).

A potential problem with the SNe ages is the high region,  $(\Omega_m, \Omega_\Lambda) \approx (0.8, 1.5)$ , which dominates the SNe fit. This region is strongly disfavored by the six other constraints considered here (see Fig. 3). These high  $(\Omega_m, \Omega_\Lambda)$  values allow lower ages than the  $t_o^{flat}$  SNe results because the slope of the iso- $t_o$  contours (Fig. 3B) is larger than the slope of the SNe contours. The  $t_o^{flat}$  results are not as subject to this problem and are the results most analogous to the result reported here, despite the fact that the SNe  $t_o^{flat}$  results are less consistent with the result reported here. There are several independent cosmological measurements which have not been included in this analysis either because a consensus has not yet been reached [gravitational lensing limits (27-30)] or because the analysis of the measurements has not been done in a way that is sufficiently free of conditioning on certain parameters [local velocity field limits (31)]. Doubts about some of the observations used here are discussed in (32). There has been speculation recently that the evidence for  $\Omega_\Lambda$  is really evidence for some form of stranger dark energy that we have incorrectly been interpreting as  $\Omega_\Lambda$ . Several workers have tested this idea. The evidence so far indicates that the cosmological constant interpretation fits the data as well as or better than an explanation based on more mysterious dark energy (4, 33, 34).

Table 2: Age estimates of our Galaxy and universe (36). “Technique” refers to the method used to make the age estimate. OC, open clusters; WD, white dwarfs; LF, luminosity function; GC, globular clusters; M/L, mass-to-light ratio; and cl evol, cluster abundance evolution. The averages are inverse variance-weighted averages of the individual measurements. The sun is not included in the disk average. “Isotopes” refers to the use of relative isotopic abundances of long-lived species as indicated by absorption lines in spectra of old disk stars. The “stellar ages” technique uses main sequence fitting and the new Hipparcos subdwarf calibration. “All” means that all six constraints in Table 1 and the CMB constraints were used in Eq. 1. “All-x” means that all seven constraints except constraint x were used in Eq. 1. Figures. 3 and 5 and the all - x results indicate a high level of agreement between constraints and the lack of dependence on any single constraint. Thus, there is a broad consistency between the ages preferred by the CMB and the six other independent constraints. Figure 2 presents all of the disk and halo age estimates.

Technique	Reference	h Assumptions	Age (Ga)	Object
Isotopes	(37)	None	$4.53 \pm 0.04$	Sun
Stellar ages	(38)	None	$8.0 \pm 0.5$	Disk OC
WD LF	(39)	None	$8.0 \pm 1.5$	Disk WD
Stellar ages	(40)	None	$9.0 \pm 1$	Disk OC
WD LF	(25)	None	$9.7^{+0.9}_{-0.8}$	Disk WD
Stellar ages	(41)	None	$12.0^{+1.0}_{-2.0}$	Disk OC
		None	$8.7 \pm 0.4$	$t_{\text{disk}}(\text{avg})$
Stellar ages	(42)	None	$11.5 \pm 1.3$	Halo GC
Stellar ages	(43)	None	$11.8^{+1.1}_{-1.3}$	Halo GC
Stellar ages	(44)	None	$12 \pm 1$	Halo GC
Stellar ages	(45)	None	$12 \pm 1$	Halo GC
Stellar ages	(46)	None	$12.5 \pm 1.5$	Halo GC
Isotopes	(47)	None	$13.0 \pm 5$	Halo stars
Stellar ages	(48)	None	$13.5 \pm 2$	Halo GC
Stellar ages	(49)	None	$14.0^{+2.3}_{-1.6}$	Halo GC
		None	$12.2 \pm 0.5$	$t_{\text{Gal}}(\text{avg})$
SNe	(4)	$0.63 \pm 0.0$	$14.5 \pm 1.0$	Universe
SNe (flat)	(4)	$0.63 \pm 0.0$	$14.9^{+1.4}_{-1.1}*$	Universe
SNe	(5)	$0.65 \pm 0.02$	$14.2 \pm 1.7$	Universe
SNe (flat)	(5)	$0.65 \pm 0.02$	$15.2 \pm 1.7*$	Universe
All	This work	$0.60 \pm 0.10$	$15.5^{+2.3}_{-2.8}$	Universe
All	This work	$0.64 \pm 0.10$	$13.5^{+3.5}_{-2.2}*$	Universe
All	This work	$0.68 \pm 0.10$	$13.4^{+1.6}_{-1.6}*$	Universe
All	This work	$0.72 \pm 0.10$	$13.3^{+1.2}_{-1.9}*$	Universe
All	This work	$0.76 \pm 0.10$	$12.3^{+1.9}_{-1.6}$	Universe
All	This work	$0.80 \pm 0.10$	$11.9^{+1.9}_{-1.6}$	Universe
All	This work	$0.64 \pm 0.02$	$14.6^{+1.6}_{-1.1}*$	Universe
All–CMB	This work	$0.68 \pm 0.10$	$14.0^{+3.0}_{-2.2}$	Universe
All–SNe	This work	$0.68 \pm 0.10$	$13.3^{+1.7}_{-1.8}$	Universe
All–M/L	This work	$0.68 \pm 0.10$	$13.3^{+1.9}_{-1.7}$	Universe
All–cl evol	This work	$0.68 \pm 0.10$	$13.3^{+1.7}_{-1.4}$	Universe
All–radio	This work	$0.68 \pm 0.10$	$13.3^{+1.7}_{-1.5}$	Universe
All–baryons	This work	$0.68 \pm 0.10$	$13.4^{+2.6}_{-1.5}$	Universe
All–Hubble	This work	None	$< 14.2$	Universe
All–CMB–SNe	This work	$0.68 \pm 0.10$	$12.6^{+3.4}_{-2.0}$	Universe

\* Also plotted in Fig. 2.

## REFERENCES

### References and Notes

1. I follow a common convention and work with dimensionless quantities. The dimensionless Hubble constant is  $h = H_0/100 \text{ km s}^{-1} \text{ Mpc}^{-1}$ , where  $H_0$  is the usual Hubble constant in units of kilometers per second per megaparsec. Both  $\Omega_m$  and  $\Omega_\Lambda$  are densities expressed in units of the critical density which is defined as  $\rho_{\text{crit}} = 3H_0^2/8\pi G$ , where  $G$  is Newton's constant. Thus,  $\Omega_m = \rho_m/\rho_{\text{crit}}$  where  $\rho_m$  is the mass density of the universe in grams per cubic centimeter. The dimensionless cosmological constant  $\Omega_\Lambda = \rho_\Lambda/\rho_{\text{crit}} = \Lambda/3H_0^2$  where  $\Lambda$  is the cosmological constant introduced in 1917 [A. Einstein, *Sitzungsber. Preuss. Akad. Wiss. Phys. Math. Kl.*, 142 (1917), English translation in *Principle of Relativity*, H.A. Lorentz et al. (Dover, New York, 1952) p. 175].
2. S.D.M. White, J.F. Navarro, A.E. Evrard, C.S. Frenk, *Nature* **366**, 429 (1993).
3. C.H. Lineweaver and D. Barbosa, *Astrophys. J.* **496**, 624 (1998).
4. S. Perlmutter *et al.*, *ibid.*, in press, (available at <http://xxx.lanl.gov/abs/astro-ph/9812133>).
5. A. G. Riess *et al.*, *Astron. J.* **116**, 1009 (1998).  $t_0^{\text{flat}} = 15.2 \pm 1.7$  results from including a flat prior in the analysis.
6. Galaxy cluster mass-to-light ratio limits are from R. Carlberg *et al.*, [*Astrophys. J.* **478**, 462 (1997)] and R. Carlberg *et al.*, [paper presented at the 33rd Rencontres de Moriond, Fundamental Parameters in Cosmology, Les Arcs, France, 17 to 24 January, 1998 (available at <http://xxx.lanl.gov/abs/astro-ph/9804312>)]. The error bars in Table 1 are conservative in the sense that they include their "worst case", 73% errors.
7. N.A. Bahcall and X. Fan, *Astrophys. J.* **504**, 1 (1998); N.A. Bahcall, X. Fan, R. Cen, *ibid.* **485**, L53 (1997). Table 1 lists their reported 95% errors, which I use as  $1\sigma$  error bars in this analysis.
8. E.J. Guerra, R.A. Daly, L. Wan, in preparation, (available at <http://xxx.lanl.gov/abs/astro-ph/9807249>). I have doubled the  $1\sigma$  errors quoted in the abstract.
9. C.H. Lineweaver, *Astrophys. J.* **505**, L69 (1998).
10. M. White, *ibid.* **506**, 495 (1998), A.M. Webster *et al.* *ibid.* **509**, 65 (1999), E. Gawiser and J. Silk, *Science* **280**, 1405 (1998).
11. M. Tegmark, *Astrophys. J.* **514**, L69 (1999). Gravitational and reionization effects were included in this analysis weakening the CMB constraints on closed models (upper right of the  $\Omega_m - \Omega_\Lambda$  plane).
12. G. Efstathiou, S.L. Bridle, A.N. Lasenby, M.P. Hobson, R.S. Ellis, *Mon. Not. R. Astron. Soc.* **303**, 47 (1999).
13. J.E. Felten and R. Isaacman, *Rev. Mod. Phys.* **58**, 689 (1986). S.M. Carroll, W.H. Press, E.L. Turner, *Annu. Rev. Astron. Astrophys.* **30**, 499 (1992) Eq. 17. There may be some ambiguity about what the "age of the universe" really means. I have used the Friedman equation derived from general relativity to extract the age of the universe. This age is the time that has elapsed since the early moments of the universe when the classical equations of general relativity became valid. In eternal inflation models [see, for example, A. Linde, *Particle Physics and Inflationary Cosmology* (Harwood Academic, Chur, Switzerland) p. 292ff (1990)] or other multiple universe scenarios ("multiverses"), the age of the universe is more complicated. If we live in a multiverse, then the age computed here refers only to the age of our bubble-like part of it.
14. A.E. Evrard, *Mon. Not. R. Astron. Soc.* **292**, 289 (1997).
15. S. Burles and D. Tytler, *Astrophys. J.* **499**, 699 (1998).

16. B.F. Madore et al. (available at <http://xxx.lanl.gov/abs/astro-ph/9812157>) report  $h = 0.72(\pm 0.05)_r[\pm 0.12]_s$  from an analysis which combines recent  $H_0$  measurements. The errors are random and systematic, respectively. F. Hoyle, G. Burbidge and J.V. Narlikar [*Mon. Not. R. Astron. Soc.*, **286**, 173, 1997] reviewed the observational literature and concluded  $h = 0.58^{+0.10}_{-0.05}$ . Both  $h = 0.65 \pm 0.10$  and  $h = 0.70 \pm 0.10$  are often cited as standard estimates [see for example (12, 18)]. I adopt  $h = 0.68 \pm 0.10$  to represent the world's efforts to measure the Hubble constant, but I also explore the  $h$  dependence of the age results in Table 2. In the likelihood,  $\mathcal{L}_{\text{Hubble}}$ , I distinguish the observationally determined estimate  $\bar{h}$  from the free parameter  $h$ .
17. Y. Yoshii, T. Tsujimoto, K. Kawara, *Astrophys. J.* **507**, L113 (1998).
18. M. Fukugita, C.J. Hogan, P.J.E. Peebles, *ibid.* **503**, 518 (1998).
19. Baryonic fraction of the mass of clusters of galaxies. Evrard (14) reports  $\Omega_m/\Omega_b = (12.5 \pm 0.7)h^{4/3}$  (independent of  $\Omega_\Lambda$ ) which becomes  $\Omega_m/\Omega_b = (12.5 \pm 3.8)h^{4/3}$  when the suggested 30% systematic error is added in quadrature. Burles & Tytler (15) report  $\Omega_b h^2 = 0.019 \pm 0.001$  but Fukugita *et al.*(18) favor a lower but larger range which includes  $\Omega_b h^2 = 0.020$ . I adopt  $\Omega_b h^2 = 0.015 \pm 0.005$ . When this is combined with the Evrard (14) result, one gets the constraint:  $\Omega_m h^{2/3} = 0.19 \pm 0.12$ .
20. These five  $\mathcal{L}_i$  have no simple analytic form.
21. These combinations prefer the upper left region of the  $(\Omega_m, \Omega_\Lambda)$  plane. I (9) have analyzed this complementarity and obtained  $\Omega_\Lambda = 0.62 \pm 0.16$  and  $\Omega_m = 0.24 \pm 0.10$ . The addition of the cluster abundance evolution measurements and improvements in the SNe measurements tightens these limits to the values given.
22.  $\mathcal{L}(h, \Omega_m, \Omega_\Lambda)$  was derived as in (9). For a discussion of taking the maximum of the likelihood, rather than doing an integral to marginalize over the nuisance variable, see (3, p. 626) and (11, Section 2.4) and references therein. The lower right of Fig. 3A shows that low  $h$  values are preferred (which correspond to older ages because  $t_o \propto 1/h$ ). This preference contrasts with the iso- $t_o$  lines (Fig. 3A) which have the younger ages in the lower right. Therefore, the three-dimensional CMB preferences will yield tighter limits on  $t_o$  than is apparent from the figure.
23. In the absence of any direct constraint on  $h$ , the data are more consistent with large values of  $h$ . For example, if no  $\mathcal{L}_{\text{Hubble}}(h)$  is used in Eq. 1, the combined data yield a lower limit  $h > 0.67$ . The corresponding age limit is  $t_o < 14.2$  Ga. No upper limit could be determined since the best fit for this data is  $h = 1.00$ , at the edge of the range explored. This preference for higher  $h$  values (lower ages) helps explain the  $h$  dependence of the results in Table 2. Results for  $0.60 \leq h \leq 0.80$  are reported in Table 2. When a small uncertainty in  $h$  was assumed (effectively conditioning on an  $h$  value), it dominated the  $h$  information from the other constraints. For example, although the central  $h$  values are the same, the results from using  $h = 0.64 \pm 0.02$  and  $h = 0.64 \pm 0.10$  are quite different: 14.6 and 13.5 Ga, respectively (Fig. 2). If  $t_o \propto 1/h$  were adhered to, there would be no difference.
24. P. Stetson, D.A. Vandenberg, M. Bolte, *Publ. Astron. Soc. Pac.* **108**, 560 (1996).
25. T.D. Oswalt, J.A. Smith, M.A. Wood, P. Hintzen, *Nature* **382**, 692 (1996); J.D. Oswalt, personal communication. Together, these references provided the age that is referred to as "Oswalt98" in Fig. 2.
26. S.P. Driver, *et al.*, *Astrophys. J.* **496**, L93 (1998). But there is no consensus on this issue. See F.R. Marleau and L. Simard, *ibid.* **507**, 585 (1998).
27. E.E. Falco, C.S. Kochanek, J.A. Munoz, *ibid.* **494**, 47 (1998).
28. Y.N. Cheng and L.M. Krauss, in preparation (available at <http://xxx.lanl.gov/abs/astro-ph/9810393>).
29. A.R. Cooray, in preparation, (available at <http://xxx.lanl.gov/abs/astro-ph/9811448>).

30. R. Quast and P. Helbig, in preparation, (available at <http://xxx.lanl.gov/abs/astro-ph/9904174>).
31. I. Zehavi, paper presented at the MPA/ESO Cosmology Conference, Evolution of Large-Scale Structure: From Recombination to Garching, 2 to 7 August 1998 (available at <http://xxx.lanl.gov/abs/astro-ph/9810246>).
32. A. Dekel, D. Burstein, S.D.M. White, in *Critical Dialogues in Cosmology* N. Turok, Ed. (World Scientific, River Edge, NJ 1998), pp. 175-191.
33. P.M. Garnavich *et al.*, *Astrophys. J.* **509**, 74 (1998).
34. S. Perlmutter, M.S. Turner, M. White, available at <http://xxx.lanl.gov/abs/astro-ph/9901052>.
35. I use SNe constraints large enough to encompass the constraints from the two SNe groups. Perlmutter *et al.* (4) report  $0.8 * \Omega_m - 0.6 * \Omega_\Lambda = -0.2 \pm 0.1$ . Evaluated at  $\Omega_\Lambda = 0$  this yields  $\Omega_m^{\Lambda=0} = -0.25 \pm 0.13$ . Assuming spatial flatness, they report  $\Omega_m^{\text{flat}} = 0.28_{-0.08}^{+0.09/+0.05}$  statistical (systematic) errors respectively. Adding the statistical and systematic errors in quadrature yields  $\Omega_m^{\text{flat}} = 0.28_{-0.09}^{+0.10}$ . The Riess *et al.* (5) constraints are from their figures 6 and 7 ("MLCS method" and "snapshot method") using either the solid or dotted contours whichever is larger (corresponding to the analysis with and without SN1997ck, respectively). This yields  $\Omega_m^{\Lambda=0} = -0.35 \pm 0.18$  and  $\Omega_m^{\text{flat}} = 0.24_{-0.10}^{+0.17}$ . I use the weighted average of these Perlmutter *et al.* (4) and Riess *et al.* (5) constraints to obtain the SNe constraints listed above. The crucial upper error bars on  $\Omega_m$  are large enough to include the constraints from either reference.
36. One would like to be less Galactocentric, but measuring the ages of even nearby extragalactic objects is difficult. See K.A. Olsen *et al.* [*Mon. Not. R. Astron. Soc.*, **300**, 665 (1998)] who find that the ages of old globular clusters in the Large Magellanic Cloud are the same age as the oldest Galactic globular clusters.
37. D.B. Guenther and P. Demarque, *Astrophys. J.* **484**, 937 (1997).
38. B. Chaboyer, E.M. Green, J. Liebert, available at <http://xxx.lanl.gov/abs/astro-ph/9812097>.
39. S.K. Leggett, M.T. Ruiz, P. Bergeron, *Astrophys. J.* **497**, 294 (1998).
40. G. Carraro, A. Vallenari, L. Girardi, A. Richichi, *Astron. Astrophys.* **343**, 825, (1999). (available at <http://xxx.lanl.gov/abs/astro-ph/9812278>).
41. R.L. Phelps, *Astrophys. J.* **483**, 826 (1997).
42. B. Chaboyer, P. Demarque, P.J. Kernan, L.M. Krauss, *ibid.* **494**, 96 (1998).
43. R.G. Gratton *et al.*, *ibid.* **491**, 749 (1997).
44. I.N. Reid, *Astron. J.* **114**, 161 (1997).
45. M. Salaris and A. Weiss, *Astron. Astrophys.* **327**, 107 (1997).
46. F. Grundahl, D.A. Vandenberg and M.T. Andersen, *Astrophys. J.* **500**, L179 (1998).
47. J.J. Cowan *et al.*, *ibid.* **480**, 246 (1998).
48. R. Jimenez, available at <http://xxx.lanl.gov/abs/astro-ph/9810311>.
49. F. Pont, M. Mayor, C. Turon, D.A. Vandenberg, *Astron. Astrophys.* **329**, 87 (1998).
50. L.M. Krauss and G.D. Starkman, in preparation, (available at <http://xxx.lanl.gov/abs/astro-ph/9902189>).
51. I thank R. De Propriis for helpful discussions on the Galactic age estimates of Table 2. I acknowledge a Vice-Chancellor's Fellowship at the University of New South Wales.